Subcarrier-Index Modulated Multicarrier Space-Time Shift Keying: Achievable Rate, Performance, and Design Guidelines

Mohammad Ismat Kadir

***Abstract*—Multicarrier (MC) space-time shift keying (STSK) relying on the concept of subcarrier-index modulated orthogonal frequency division multiplexing (SIM-OFDM) is proposed. In conventional MC-STSK system, the performance erosion of STSK in dispersive channels is mitigated by employing OFDM. The SIM-OFDM aided MC-STSK activates a specified limited number of subcarriers for transmitting the STSK codewords. The indices of the activated subcarriers provide additional multiplexing gain. A new receiver architecture, which uses the single-stream maximum-likelihood (ML) detector of STSK and the subcarrier activation principle of SIM-OFDM, is designed. A soft decision logarithmic likelihood ratio (LLR) based detector is also conceived. Helpful design guidelines are provided for the system. The achievable rate, complexity, and performance of the system are analytically quantified and verified with the aid of numerical simulations. The system is capable of overcoming the impairments imposed by wideband channels, is benefited from index modulation as well as from STSK. The scheme exhibits an improved error performance compared to the classic OFDM-based STSK as a result of the more reliable detection of the subcarrier index bits.**

***Index Terms*—Space-time shift keying (STSK), orthogonal frequency division multiplexing (OFDM), subcarrier index modulation, multiple-input multiple-output (MIMO).**

I. Introduction

THE concept of subcarrier index modulation (SIM) aided orthogonal frequency division multiplexing (OFDM) [1]–[4] has emerged as a beneficial technique. The idea is to activate a subset of OFDM subcarriers rather than activating all the subcarriers available. The indices of the subcarriers activated facilitate the transmission of extra source information. The pioneering study on SIM-OFDM was carried out in [1] and was followed by [2]–[6]. A detailed transceiver architecture of the SIM-OFDM system was proposed in [2] and extended to the multiple-input multiple-output (MIMO) scenario in [3].

On the other hand, space-time shift keying (STSK) [7], [8] attracted substantial research interests as a beneficial MIMO scheme. STSK subsumes the previous MIMO concepts of spatial multiplexing (SMUX) [9], space-time block code (STBC) [10], linear dispersion code (LDC) [11], [12], spatial modulation (SM) [13] and space shift keying (SSK) [14]. The motivation of STSK came from the flexible diversity-multiplexing trade-off (DMT) [15] provided by LDC as well as from the low-complexity design of SM and SSK. While SMUX is capable of providing spatial multiplexing gain and STBC is conceived for providing transmit diversity gain, LDC is capable of striking a flexible DMT, albeit at the cost of a substantially-increased decoding complexity. As a design alternative, SM/SSK activates a single antenna element (AE) and the index of the AE activated can provide additional multiplexing gain. SM/SSK imposes a significantly low decoding complexity. Against these conflicting design ideas, STSK was proposed for striking a flexible DMT, whilst the decoding complexity is significantly reduced [8]. The basic idea behind this reduction in complexity is that STSK activates a single LDC-style dispersion matrix (DM) at every signaling interval. Thus both SM/SSK and STSK may be regarded as the 'index modulation (IM)' schemes. SM/SSK [14], [16], [17] employs the AE index as an information-bearing entity and may be called the 'spatial IM' scheme, whereas STSK uses the DM index for conveying additional information and may be referred to as the 'DM IM' scheme. As a benefit of the employment of the DMs, STSK [7], [8] can disperse the information bits to both the spatial and time dimensions. Consequently, STSK is capable of achieving both the multiplexing gain and the spatial as well as time domain diversity gain.

Motivated by the additional multiplexing gain provided by the AE index of SM and by the DM index of STSK, a generalized SM (GSM) [18] and a generalized STSK (GSTSK) [19] scheme were also proposed for increasing the achievable spectral efficiency. In GSM, a number of transmit AEs rather than a single AE are selectively activated at a time. In GSTSK, a number of DMs are activated simultaneously for the transmission of more information bits over the spatial- and time domain. The GSM and the GSTSK scheme, however, attain this increased spectral efficiency at the cost of a modest increase in complexity as well as the inter-element interference (IEI). Thus the GSM and the GSTSK schemes provide a fair compromise between the attainable spectral efficiency and complexity as well as IEI

Manuscript received March 23, 2018; revised September 8, 2018 and November 6, 2018; accepted December 5, 2018. Date of publication January 3, 2019; date of current version March 14, 2019. The work of M. I. Kadir was supported by the Commonwealth Scholarship Commission's Academic Fellowship. The review of this paper was coordinated by Y. L. Guan.

The author was with the School of ECS, University of Southampton, Southampton SO17 1BJ, U.K. He is now with the Department of Electronics and Communication Engineering, Khulna University, Khulna 9208, Bangladesh (e-mail: ismat.kadir@ece.ku.ac.bd).

Digital Object Identifier 10.1109/TVT.2019.2890794

0018-9545 © 2019 IEEE. Personal use is permitted, but republication/redistribution requires IEEE permission.
See http://www.ieee.org/publications_standards/publications/rights/index.html for more information.

Authorized licensed use limited to: Khulna University. Downloaded on October 17,2026 at 10:20:16 UTC from IEEE Xplore. Restrictions apply.

with its SMUX counterpart. In line with the developments on the SM, GSM, STSK and the SIM-OFDM, generalized space- and frequency index modulation (GSFIM) [20] and space-time frequency index modulation (STFIM) [21] were also proposed.

Although SM, STSK, GSM and GSTSK provide satisfactory performance in frequency-flat channels, the performance degrades in frequency-selective wireless channels. To mitigate the performance degradation of STSK in frequency-selective channels, a range of multicarrier (MC) STSK [8], [22] schemes were proposed. These schemes rely on MC technique for slowing down the transmission rate over each subcarrier. As a result, the individual subchannels experience frequency-flat fading and the performance erosion of the schemes in frequency-selective channels is mitigated. Despite these developments on MC-STSK [8] and on SIM-OFDM [2], [4], a MC-STSK system relying on the SIM technique along with a comprehensive analysis of its error performance and achievable rate still remains as an open problem.

Against this backdrop, a SIM-OFDM-aided MC-STSK is proposed which employs both the subcarrier- and the DM indices as additional means of conveying information. The contributions of the paper may be summarized as follows:

1) A multicarrier (MC) STSK system relying on the SIM-OFDM technique is conceived and the transceiver architecture of the system is detailed.
2) A single-stream maximum likelihood (ML) detector is designed for the system, taking the subcarrier activation principle into account. Furthermore, a reduced-complexity log-likelihood (LLR) detector using the philosophy of [2] is conceived for the SIM-OFDM-STSK.
3) The achievable rate of the scheme and the complexity associated with the detectors are quantified.
4) An upper-bound on the bit-error-probability (BEP) of the SIM-OFDM-STSK system is analytically derived with the aid of the bound on the pairwise error probability (PEP) and considering the legitimate subcarrier activation patterns of the SIM-OFDM system. The analytical BEP is also verified against the simulation results.
5) Finally, some helpful design guidelines for the SIM-OFDM STSK system are provided.

Multiplying multiple modulation symbols by DMs may be called a GSTSK-based IM technique, which may be capable of providing additional multiplexing gain [19], [23].

A. Outline

The paper is organized as follows. In Section II, the transceiver architecture of the SIM-OFDM-aided MC STSK system is detailed. The achievable rate and the complexity imposed by the SIM-OFDM-STSK scheme are quantified in Section III. Section IV deals with the error performance of the system and provides some helpful design guidelines. In Section V the proposed system is investigated using numerical simulations. Finally, the paper is concluded in Section VI.

B. Notations

In general, boldface letter, for example $\boldsymbol{A}$, is used to represent a matrix or a vector, while $\boldsymbol{A}^T$, $\boldsymbol{A}^H$, $\mathrm{tr}(\boldsymbol{A})$, $\mathrm{vec}(\boldsymbol{A})$, $(\boldsymbol{A})_q$, $|\boldsymbol{A}|$ and $\|\boldsymbol{A}\|$ denote the matrix transpose, the Hermitian transpose, the trace, the column-wise vectorial stacking operator, the q-th column, the determinant and the Euclidean norm of $\boldsymbol{A}$, respectively. The operator $\otimes$ represents the Kronecker product, $\boldsymbol{A} \oplus \boldsymbol{B}$ the exclusive OR on $\boldsymbol{A}$ and $\boldsymbol{B}$, $\boldsymbol{I}_T$ the $T \times T$ identity matrix, $\mathbf{0}_v$ the column vector of zeros only, $\mathbf{1}_v$ the column vector of ones only and $\mathbf{0}_{M\times T}$ the $M \times T$ zero matrix. $\Pr(\cdot)$ denotes the probability of '$\cdot$', while $\boldsymbol{\mathcal{F}}_{N_c}$ and $\boldsymbol{\mathcal{F}}_{N_c}^H$ denote the N_c-point discrete Fourier transform (DFT) matrix and the N_c-point inverse DFT (IDFT) matrix, respectively.

II. System Overview of the SIM-OFDM-Aided STSK

Fig. 1 shows the schematic of the SIM-OFDM based MC-STSK transmitter, which has M transmit- and N receive AEs and which communicates over frequency-selective Rayleigh fading channel. A total of N_c subcarriers are employed for the transmission of the STSK space-time (ST) codewords, while N_p subcarriers are activated by the SIM-OFDM scheme.

A. The Transmitter Model

As shown in Fig. 1, b source bits are transmitted in an OFDM block duration using M transmit AEs over T time slots. The b bits are divided into K parallel subblocks of $(b_1 + b_2 + b_3)$ bits, such that $b = K(b_1 + b_2 + b_3)$. Each of the subblocks are then split into three parallel bit-sequences of b_1, b_2 and b_3 bits, respectively. Note that the b_1 and b_2 bits are used to select the indices of the DM activated and of the subcarriers activated, respectively and may be called as the 'index bits', whereas the b_3 bits are mapped to the constellation symbols [7]. Furthermore, after the serial-to-parallel operation, the available N_c subcarriers are divided into K subblocks of N_b subcarriers each, where $N_c = KN_b$. Similarly the N_p subcarriers to be selected by the SIM scheme are also divided into the K number of N_a subcarriers each, where $N_p = KN_a$. Specifically, the b_1 and b_3 bits from each of the bit splitters are utilized to generate the N_a STSK codewords $\boldsymbol{S}^k[n_a] \in \mathbb{C}^{M\times T} \quad (n_a = 1, 2, \ldots, N_a)$ for each of the parallel subblocks $k = 1, 2, \ldots, K$ according to the relationship [7]: $\boldsymbol{S}^k[n_a] = s_l^k[n_a]\boldsymbol{A}_q^k[n_a]$, where $s_l^k[n_a]$ is the $\mathcal{L}$-PSK/QAM symbol mapped by $\log_2 \mathcal{L}$ bits of source information, $\boldsymbol{A}_q^k[n_a]$ is the activated DM from Q such pre-assigned matrices $\boldsymbol{A}_q \in \mathbb{C}^{M\times T} \quad (q = 1, ..., Q)$ as determined by the $\log_2 Q$ DM index bits. The DMs are optimized for minimizing the PEP or for maximizing the capacity of the STSK scheme under the power constraint [7], [11] given by: $\mathrm{tr}(\boldsymbol{A}_q^H \boldsymbol{A}_q) = T$. The corresponding STSK scheme [7], [8] may be uniquely described by the $(M, N, T, Q, \mathcal{L})$ parameters.

The number of bits b_1 and b_3 are so selected that $b_1 = N_a \log_2 Q$, $b_2 = \lfloor \log_2 \binom{N_b}{N_a} \rfloor$ and $b_3 = N_a \log_2 \mathcal{L}$. The b_2 bits of the $k-$th subblock are mapped to the integer set $\mathfrak{p}^k$ of the

Authorized licensed use limited to: Khulna University. Downloaded on October 17,2026 at 10:20:16 UTC from IEEE Xplore. Restrictions apply.

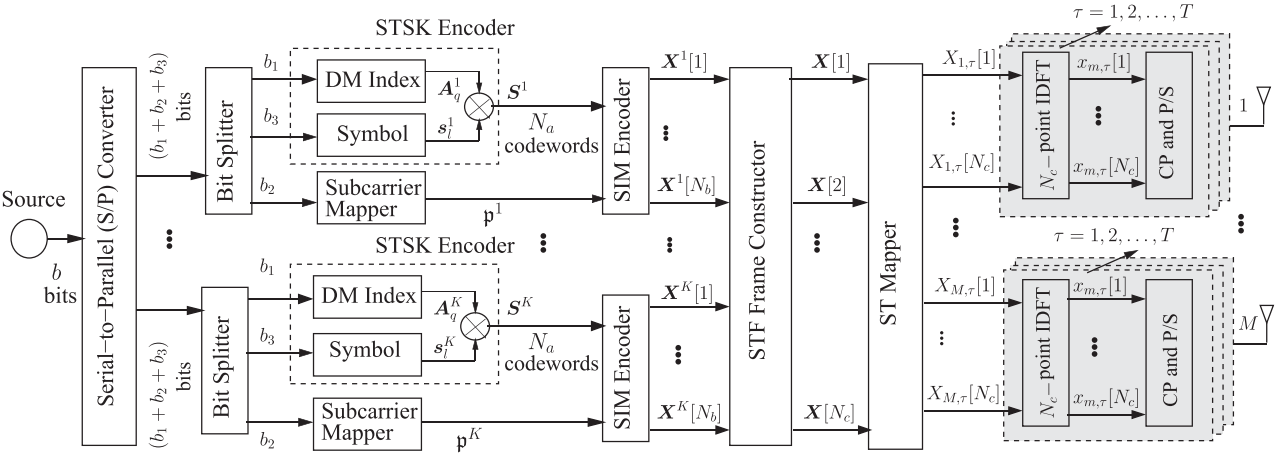


Fig. 1. The block diagram of the SIM-OFDM-aided STSK transmitter.

activated subcarrier indices by the 'Subcarrier Mapper' of Fig. 1. Furthermore, since the b_2 bits may be mapped to the set $\mathfrak{p}^k$ of subcarrier indices in 2^{b_2} ways, there are 2^{b_2} legitimate $\mathfrak{p}^k$ values denoted by $\mathfrak{p}_i^k$ $(i = 1, 2, \ldots, 2^{b_2})$.

B. The SIM-OFDM Encoding

After the bit mapping to the STSK codewords and to the subcarrier indices, N_a codewords represented by $\boldsymbol{S}^k = \{\boldsymbol{S}^k[1], \boldsymbol{S}^k[2], \ldots, \boldsymbol{S}^k[N_a]\}$ and the subcarrier activation pattern (SAP) denoted by $\mathfrak{p}^k$ are passed through the 'SIM Encoder' of Fig. 1. The 'SIM Encoder' maps the N_a codewords to N_b ST matrices $\boldsymbol{X}^k[1]$, $\boldsymbol{X}^k[2]$, $, \ldots, \boldsymbol{X}^k[N_b]$ in every subblock $k = 1, 2 \ldots, K$. The SIM scheme [2], [4] may be uniquely defined by the (N_b, N_a, K) parameters.

Having mapped the N_a codewords to the N_b subcarriers, $(b_1 + b_2 + b_3)$ bits of each parallel subblock form a space-time-frequency (STF) frame. The STF frame may be expressed by a block matrix [24] $\boldsymbol{X}^k := [\boldsymbol{X}^k[1] \quad \boldsymbol{X}^k[2] \quad \cdots \quad \boldsymbol{X}^k[N_b]] \quad \in \mathbb{C}^{M \times N_b T}$. The 'STF Frame Constructor' of Fig. 1 collects the STF frames of all the parallel subblocks. The STF frames constitute an OFDM STF codeword. The STF codeword may be considered as a combination of N_c ST codewords placed in parallel across the frequency-domain (FD) as shown in Fig. 2 and may be expressed by the block matrix [24] given by

$$\boldsymbol{X} := [\boldsymbol{X}[1] \quad \boldsymbol{X}[2] \quad \cdots \quad \boldsymbol{X}[N_c]] \quad \in \mathbb{C}^{M \times N_c T} \qquad (1)$$

where among the N_c ST matrices, N_p are the STSK codewords and the remaining $(N_c - N_p)$ are $M \times T$ zero matrices $\mathbf{0}_{M \times T}$. The STF codeword is then mapped by the 'ST Mapper' to the M AEs over T time slots for appropriate OFDM processing.

As proposed in [2], N_a out of N_b subcarriers may be chosen by using a look-up table (LUT) or by a combinatorial method. The LUT method consumes exponentially increasing memory space with the increase in b_2 bits [1]. On the other hand, the

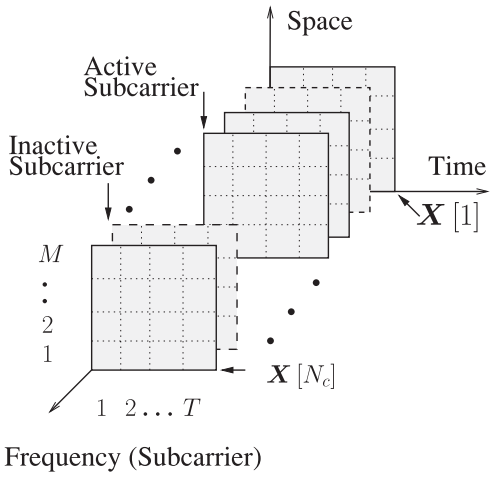


Fig. 2. Space-time-frequency (STF) codeword of the SIM-OFDM-STSK system viewed as a parallel combination of N_c ST matrices.

combinatorial method is proposed for larger number of subcarriers [2]. Hence, the one-to-one correspondence between the b_2 bits and the SAP is generated as a binary matrix [1]:

$$\boldsymbol{P}^k_{N_a, N_b} \triangleq \begin{bmatrix} \mathbf{1}_v & \boldsymbol{P}^k_{N_a-1, N_b-1} \\ \mathbf{0}_v & \boldsymbol{P}^k_{N_a, N_b-1} \end{bmatrix} \in \mathbb{Z}^{\binom{N_b}{N_a} \times N_b}, \qquad (2)$$

where the column vectors $\mathbf{1}_v$ and $\mathbf{0}_v$ have lengths $\binom{N_b-1}{N_a-1}$ and $\binom{N_b-1}{N_a}$, respectively. The matrix $\boldsymbol{P}^k_{N_a, N_b}$ can be constructed recursively, terminating in either $\boldsymbol{P}^k_{N_S, N_S}$ (a square matrix of ones only) or in $\boldsymbol{P}^k_{0, N_S}$ (containing zeros only) [1].

To exemplify the mapping of source bits to STSK codewords as well as to the SAPs, let us consider a SIM-OFDM-STSK with $N_c = 64$, $N_p = 32$, $Q = 2, \mathcal{L} = 2$ and $K = 32$. With these parameter values, we have $N_b = 2$, $N_a = 1$ yielding a 2×2 binary matrix $\boldsymbol{P}^k_{1,2} = \left[\begin{smallmatrix} 1 & 0 \\ 0 & 1 \end{smallmatrix}\right] \in \mathbb{Z}^{2 \times 2}$. The two row vectors $\boldsymbol{p}_1^k = [1\ 0]$ and $\boldsymbol{p}_2^k = [0\ 1]$ correspond to the two SAPs $\mathfrak{p}_1^k = \{1\}$ and $\mathfrak{p}_2^k = \{2\}$, respectively. This scheme is thus capable of transmitting $N_a \log_2(Q \cdot \mathcal{L}) + \lfloor \log_2 \binom{N_b}{N_a} \rfloor = 3$ bits per

Authorized licensed use limited to: Khulna University. Downloaded on October 17,2026 at 10:20:16 UTC from IEEE Xplore. Restrictions apply.

TABLE I
MAPPING OF SIM-OFDM-STSK BITS TO STF FRAMES FOR 3 BITS PER SUBBLOCK, $N_b = 2, N_a = 1, Q = 2$, AND $\mathcal{L} = 2$

Input bits per block			Mapped DM, Subcarrier index and BPSK symbol			Mapped STF frame
b_1	b_2	b_3	$\boldsymbol{A}_q^k$	$\mathfrak{p}^k$	s_l^k	$\boldsymbol{X}^k$:
0	0	0	$\boldsymbol{A}_1$	$\mathfrak{p}_1^k = \{1\}$	$+1$	$[+\boldsymbol{A}_1 \quad \boldsymbol{0}_{M\times T}]$
0	0	1	$\boldsymbol{A}_1$	$\mathfrak{p}_1^k = \{1\}$	-1	$[-\boldsymbol{A}_1 \quad \boldsymbol{0}_{M\times T}]$
0	1	0	$\boldsymbol{A}_1$	$\mathfrak{p}_2^k = \{2\}$	$+1$	$[\boldsymbol{0}_{M\times T} \quad +\boldsymbol{A}_1]$
0	1	1	$\boldsymbol{A}_1$	$\mathfrak{p}_2^k = \{2\}$	-1	$[\boldsymbol{0}_{M\times T} \quad -\boldsymbol{A}_1]$
1	0	0	$\boldsymbol{A}_2$	$\mathfrak{p}_1^k = \{1\}$	$+1$	$[+\boldsymbol{A}_2 \quad \boldsymbol{0}_{M\times T}]$
1	0	1	$\boldsymbol{A}_2$	$\mathfrak{p}_1^k = \{1\}$	-1	$[-\boldsymbol{A}_2 \quad \boldsymbol{0}_{M\times T}]$
1	1	0	$\boldsymbol{A}_2$	$\mathfrak{p}_2^k = \{2\}$	$+1$	$[\boldsymbol{0}_{M\times T} \quad +\boldsymbol{A}_2]$
1	1	1	$\boldsymbol{A}_2$	$\mathfrak{p}_2^k = \{2\}$	-1	$[\boldsymbol{0}_{M\times T} \quad -\boldsymbol{A}_2]$

subblock. Table I illustrates the bit mapping of the scheme to the STF frames.

Applying the N_c-point IDFT on the codeword symbols, the TD signal may be expressed as $\boldsymbol{x}: = [\boldsymbol{x}\,[1] \quad \boldsymbol{x}\,[2] \ldots \boldsymbol{x}\,[N_c]]$. Cyclic prefix (CP) of appropriate length is added for eliminating the effects of inter-symbol interference (ISI) and the resultant signal is transmitted over the M transmit AEs.

C. The Receiver Model

Let us assume each link of the MIMO system to be frequency-selective and the TD channel impulse response (CIR) of the (n,m)-th link to be given by $\boldsymbol{h}_{n,m} \quad (n = 1, 2, \ldots, N), (m = 1, 2, \ldots, M)$. The FD MIMO channel matrix corresponding to subcarrier n_c is denoted by $\tilde{\boldsymbol{H}}[n_c]$, whose (n,m)-th entry $(\tilde{H}[n_c])_{n,m} = \tilde{h}_{n,m}[n_c]$ is obtained from $\tilde{\boldsymbol{h}}_{n,m} = \boldsymbol{\mathcal{F}}_{N_c}\{\boldsymbol{h}_{n,m}\}$. The FD MIMO output, after the removal of the CP and the N_c-point DFT processing on the received signal, may be written as [8]:

$$\boldsymbol{Y}[n_c] = \tilde{\boldsymbol{H}}[n_c]\boldsymbol{X}[n_c] + \boldsymbol{V}[n_c], \quad (n_c = 1, 2, \ldots, N_c) \quad (3)$$

where $\boldsymbol{V}[n_c]$ is the FD additive white Gaussian noise and

$$\boldsymbol{Y}[n_c] \in \mathbb{C}^{N\times T} \quad \boldsymbol{X}[n_c] \in \mathbb{C}^{M\times T}$$
$$\boldsymbol{V}[n_c] \in \mathbb{C}^{N\times T} \quad \tilde{\boldsymbol{H}}[n_c] \in \mathbb{C}^{N\times M}.$$

Equation (3) can be re-written by the linearization procedure of [7] and [12] as:

$$\overline{\boldsymbol{Y}}[n_c] = \overline{\tilde{\boldsymbol{H}}}[n_c]\boldsymbol{\chi}\boldsymbol{\mathcal{K}}[n_c] + \overline{\boldsymbol{V}}[n_c], \quad (n_c = 1, 2, \ldots, N_c) \quad (4)$$

where we have,

$$\overline{\boldsymbol{Y}}[n_c] = \text{vec}(\boldsymbol{Y}[n_c]) \in \mathbb{C}^{NT\times 1} \quad (5)$$

$$\overline{\tilde{\boldsymbol{H}}}[n_c] = \boldsymbol{I}_T \otimes \tilde{\boldsymbol{H}}[n_c] \in \mathbb{C}^{NT\times MT} \quad (6)$$

$$\boldsymbol{\chi} = [\text{vec}(\boldsymbol{A}_1), \ldots, \text{vec}(\boldsymbol{A}_Q)] \in \mathbb{C}^{MT\times Q} \quad (7)$$

$$\overline{\boldsymbol{V}}[n_c] = \text{vec}(\boldsymbol{V}[n_c]) \in \mathbb{C}^{NT\times 1}. \quad (8)$$

Furthermore, the vector $\boldsymbol{\mathcal{K}}[n_c]$ of (4) is defined [7] by

$$\boldsymbol{\mathcal{K}}[n_c] \triangleq [0, 0, ..., 0, s_l, 0, 0, ..., 0]^T \in \mathbb{C}^{Q\times 1}, \quad (9)$$

where the constellation symbol s_l is placed only in the $q[n_c]$-th position and $q[n_c]$ is the DM index on subcarrier n_c.

The receiver detects the source information by estimating the bits mapped to the subcarrier indices as well as those mapped to the STSK DM indices and the constellation symbols.

1) Single-Stream ML Detector: Unlike the single-stream ML detector of [7], the ML detector for the SIM-OFDM-STSK scheme estimates the source information from the indices to the subcarriers activated, from the indices to the DM activated and from the constellation symbol for the k-th subblock indicated by $\hat{\mathfrak{p}}^k, \hat{q}^k$ and $\hat{l}^k$, respectively. Considering all the relevant subcarriers for the specific parallel subblock k, the ML detector may be formulated [7], [14] as:

$$\left(\hat{\mathfrak{p}}^k, \hat{q}^k, \hat{l}^k\right) = \arg\min_{\mathfrak{p},q,l} \sum_{n_a=1}^{N_a} \left\| \overline{\boldsymbol{Y}}^k[n_a] - s_l \left(\overline{\tilde{\boldsymbol{H}}}^k[n_a]\boldsymbol{\chi}\right)_q \right\|^2. \quad (10)$$

As quantified in Section III-B, the single-stream ML detector of (10) imposes a high decoding complexity.

2) Reduced-Complexity LLR Detector: For the sake of reducing the high computational complexity of the ML detector, a soft-decision LLR based detector is conceived. The LLR of the n_c-th subcarrier $\lambda\,[n_c]$ may be defined as [2], [23]:

$$\lambda\,[n_c] \triangleq \ln \frac{\sum_{i=1}^{(Q\cdot\mathcal{L})} \Pr\left(\boldsymbol{\mathcal{K}}[n_c] = \boldsymbol{\mathcal{K}}_i \mid \overline{\boldsymbol{Y}}[n_c]\right)}{\Pr\left(\boldsymbol{\mathcal{K}}[n_c] = \boldsymbol{0}_{Q\times 1} \mid \overline{\boldsymbol{Y}}[n_c]\right)}, \quad (11)$$

where $\boldsymbol{\mathcal{K}}_i$ is one of the $(Q\cdot\mathcal{L})$ legitimate values of $\boldsymbol{\mathcal{K}}[n_c]$ defined in (9). Consider that $\sum_{i=1}^{(Q\cdot\mathcal{L})} \Pr\left(\boldsymbol{\mathcal{K}}[n_c] = \boldsymbol{\mathcal{K}}_i\right) = N_a/N_b$ and $\Pr\left(\boldsymbol{\mathcal{K}}[n_c] = \boldsymbol{0}_{Q\times 1}\right) = (N_b - N_a)/N_b$. Denoting the FD noise variance by N_0 and using $N_p = N_c/2$, we have [2]:

$$\lambda\,[n_c] = \frac{\left\|\overline{\boldsymbol{Y}}[n_c]\right\|^2}{N_0} + \ln\left(\sum_{i=1}^{(Q\cdot\mathcal{L})} \exp\left(-\frac{\left\|\overline{\boldsymbol{Y}}[n_c] - \overline{\tilde{\boldsymbol{H}}}[n_c]\boldsymbol{\chi}\boldsymbol{\mathcal{K}}_i[n_c]\right\|^2}{N_0}\right)\right). \quad (12)$$

The LLRs of all the subcarriers may be computed by employing the Jacobian logarithm based approximation [25] on (12). The LLR-based detector considers the subcarriers corresponding to the highest N_p LLR values to be activated. Having detected the subcarrier index bits, the estimation of the bits mapped to

Authorized licensed use limited to: Khulna University. Downloaded on October 17,2026 at 10:20:16 UTC from IEEE Xplore. Restrictions apply.

the DM indices and to the constellation symbols are straightforward. This may be performed using the single-stream ML detector of [7] over the FD codewords:

$$\left(\hat{q},\hat{l}\right)=\arg\min_{q,l}\left\|\overline{\boldsymbol{Y}}^{k}[n_a]-s_l\left(\overline{\tilde{\boldsymbol{H}}}^{k}[n_a]\boldsymbol{\chi}\right)_q\right\|^2. \quad (13)$$

III. Achievable Rate and Complexity

In this section, the achievable transmission rate and the complexity associated with the detectors are investigated.

A. Achievable Rate

In SIM-OFDM STSK, $(b_1+b_3)=N_a\log_2(Q\cdot\mathcal{L})$ bits are used for generating N_a STSK codewords for each of the K subblocks, while $b_2=\left\lfloor\log_2\binom{N_b}{N_a}\right\rfloor$ bits are employed for selecting N_a subcarriers from N_b subcarriers. The normalized overall throughput for the system [26] is thus given by

$$R=\frac{K}{N_cT}\left(N_a\log_2(Q\cdot\mathcal{L})+\left\lfloor\log_2\binom{N_b}{N_a}\right\rfloor\right)\quad\text{bits/s/Hz}. \quad (14)$$

Using Stirling's approximation for factorials [20], [27], the upper and lower bounds of the normalized achievable rate of the SIM-OFDM-STSK may be formulated as [20], [23]:

$$R\le\frac{K}{N_cT}\left[f(N_b,N_a,Q,\mathcal{L})+\log_2\frac{e\sqrt{N_b}}{2\pi\sqrt{N_b-1}}\right] \quad (15)$$

and

$$R>\frac{K}{N_cT}\left[f(N_b,N_a,Q,\mathcal{L})+\log_2\frac{\sqrt{2\pi}}{e^2\sqrt{N_b}}\right] \quad (16)$$

respectively, where the function $f(N_b,N_a,Q,\mathcal{L})$ is defined by $f(N_b,N_a,Q,\mathcal{L})\triangleq N_b\log_2N_b-N_a\log_2N_a-(N_b-N_a)\log_2(N_b-N_a)+N_a\log_2(Q\cdot\mathcal{L})$.

The upper and the lower bounds on the normalized maximum achievable rate $R^{\max}$ may also be found [20], [23] as

$$R^{\max}\le\frac{K}{N_cT}\left[N_b\log_2(Q\cdot\mathcal{L}+1)+\log_2\frac{e\sqrt{N_b}}{2\pi\sqrt{N_b-1}}\right] \quad (17)$$

and

$$R^{\max}\ge\frac{K}{N_cT}\left[N_b\log_2(Q\cdot\mathcal{L}+1)+\log_2\frac{\sqrt{2\pi}}{e^2\sqrt{N_b}}\right] \quad (18)$$

respectively, when $N_b\ge2(Q\cdot\mathcal{L})$.

B. Complexity

The complexity associated with the relevant detectors is evaluated in terms of the real-valued multiplication operations (RMOs) required per bit of information transmitted.

The ML detector of (10) has a search space of $2^{\left\lfloor\log_2\binom{N_b}{N_a}\right\rfloor}$ for the SAP per subblock. For each $\boldsymbol{p}^k$, the detector has to search over N_a STSK codewords involving the search for the DM-index q^k and the constellation symbol s_l^k. Hence the complexity associated with the ML detector of (10) for a fast fading channel is given by [7], [23]

$$C_{\text{ML}}=\frac{N_a\left(4MNT^2Q+6NTQ\mathcal{L}\right)2^{\left\lfloor\log_2\binom{N_b}{N_a}\right\rfloor}}{N_a\log_2(Q\cdot\mathcal{L})+\left\lfloor\log_2\binom{N_b}{N_a}\right\rfloor}. \quad (19)$$

The computation of LLRs employing (12) involves $\left(4MNT^2Q+6NTQ\mathcal{L}+2NT+Q\mathcal{L}+1\right)$ RMOs for each subcarrier in addition to those associated with the computation of (13). Hence the complexity of the reduced-complexity soft-decision detector of the SIM-OFDM-STSK is given by

$$C_{\text{LLR}}=\frac{\left(4MNT^2Q+6NTQ\mathcal{L}\right)(N_c+1)+N_c(2NT+Q\mathcal{L}+1)}{KN_a\log_2(Q\cdot\mathcal{L})+K\left\lfloor\log_2\binom{N_b}{N_a}\right\rfloor} \quad (20)$$

for the fast-fading channel [7], [23]. The complexities associated with the relevant systems are tabulated in Table II.

IV. Error Performance and Design Guidelines

In this section, the error performance of SIM-OFDM-STSK is investigated and helpful design guidelines are provided.

A. Error Performance

Under the assumption of the availability of channel state information (CSI) at the receiver and each link between any transmit and receive AE pair of the STSK system experiencing zero-mean, complex Gaussian noise, the average PEP of misinterpreting an STSK codeword $\boldsymbol{X}$ for $\boldsymbol{X}'$ by the ML detector of (10) is upper-bounded by [12]

$$\Pr(\boldsymbol{X}\to\boldsymbol{X}')\le\frac{1}{\left|\boldsymbol{I}_{M\cdot N}+\left(\frac{E_S}{4N_0}\right)\boldsymbol{\Lambda}\otimes\boldsymbol{I}_N\right|}, \quad (21)$$

where E_S and $N_0/2$ denote the signal power and the noise variance per dimension respectively and $\boldsymbol{\Lambda}=(\boldsymbol{X}-\boldsymbol{X}')(\boldsymbol{X}-\boldsymbol{X}')^H$. Equation (21) may be re-written at high signal-to-noise ratio (SNR) as [12]:

$$\Pr(\boldsymbol{X}\to\boldsymbol{X}')\le\left(\prod_{i=1}^{r}\lambda_i\right)^{-N}\left(\frac{E_S}{4N_0}\right)^{-rN}, \quad (22)$$

where r and λ_i indicate the rank and the non-zero eigenvalues, respectively, of $\boldsymbol{\Lambda}$. Let both $\boldsymbol{X}$ and $\boldsymbol{X}'$ belong to the legitimate set $\mathbb{A}_x$ of codewords. The diversity and the coding advantage [24], [28] are then expressed by the minimum products $\mathcal{G}_d=\min_{\boldsymbol{X}\neq\boldsymbol{X}'\in\mathbb{A}_x}(r\cdot N)$ and $\mathcal{G}_c=\min_{\boldsymbol{X}\neq\boldsymbol{X}'\in\mathbb{A}_x}\left(\prod_{i=1}^{r}\lambda_i\right)^N$, respectively. The actual PEP of the codewords corresponding to a single subcarrier as given by (22) is dependent on a number of parameters namely the choice of $\boldsymbol{X}$ and $\boldsymbol{X}'$, the channel parameters, and the design of the DMs [12].

In the context of the ML detector of the SIM-OFDM-STSK system, several things are worth mentioning here:

Authorized licensed use limited to: Khulna University. Downloaded on October 17,2026 at 10:20:16 UTC from IEEE Xplore. Restrictions apply.

TABLE II
DECODING COMPLEXITY OF THE RELEVANT SCHEMES IN FAST-FADING CHANNEL

Scheme	Complexity
ML detector of the STSK scheme of [7] and of the OFDM-aided STSK scheme of [8]	$\frac{4MNT^2Q+6NTQ\mathcal{L}}{\log_2(Q\cdot\mathcal{L})}$
ML detector of (10) for the SIM-OFDM-STSK system	$\frac{N_a\left(4MNT^2Q+6NTQ\mathcal{L}\right)2^{\left\lfloor\log_2\binom{N_b}{N_a}\right\rfloor}}{N_a\log_2\left(Q\cdot\mathcal{L}\right)+\left\lfloor\log_2\binom{N_b}{N_a}\right\rfloor}$
Reduced-complexity soft detector employing (12) and (13) for the SIM-OFDM-STSK system	$\frac{\left(4MNT^2Q+6NTQ\mathcal{L}\right)(N_c+1)+N_c\left(2NT+Q\mathcal{L}+1\right)}{KN_a\log_2\left(Q\cdot\mathcal{L}\right)+K\left\lfloor\log_2\binom{N_b}{N_a}\right\rfloor}$

1) The ML detector of (10) jointly estimates the bits mapped to the N_a STSK codewords and those mapped to the subcarrier activation vector $\boldsymbol{p}^k$ of a subblock.
2) Detection errors may occur in two different ways. Firstly, if the SAP of a subblock is not correctly detected, then both the b_2 bits mapped to the activated subcarriers and the b_1 and b_3 bits mapped to the STSK codewords will be affected. Secondly, if the SAP is correctly detected, the codewords may still be incorectly detected affecting only the b_1 and b_3 bits.
3) In order to estimate the SAP, we consider a zero matrix $\mathbf{0}_{M\times T}$ in addition to the codeword $\boldsymbol{X}$ for representing the inactive subcarriers.

Misdecoding an STSK codeword as $\mathbf{0}_{M\times T}$ results in an incorrect SAP detection. The number $d_{i,j}$ of incorrecly detected subcarriers for a specific $\boldsymbol{p}_i^k$ misdecoded as $\boldsymbol{p}_j^k$ may be expressed [29] by

$$d_{i,j}=\sum_{k=1}^{N_b}\left(\boldsymbol{p}_i^k\oplus\boldsymbol{p}_j^k\right), \tag{23}$$

where $1\le i\le 2^{\left\lfloor\log_2\binom{N_b}{N_a}\right\rfloor}$, and $1\le j\le\binom{N_b}{N_a},\ (j\neq i)$.

Let us denote the PEP corresponding to the pairwise error event of $(\boldsymbol{X}\to\boldsymbol{X}')$ and $(\boldsymbol{X}\to\mathbf{0}_{M\times T})$ as P_x and P_0, respectively, the probability of $d_{i,j}$ subcarriers to be incorrectly detected may be expressed as [29]:

$$P_{i,j}=(P_0)^{d_{i,j}}\ . \tag{24}$$

Let us further denote the number of index bit errors corresponding to the subcarrier activation error event of $\left(\boldsymbol{p}_i^k\to\boldsymbol{p}_j^k\right)$ by $e_i\left(\boldsymbol{p}_i^k,\boldsymbol{p}_j^k\right)$, and the number of bit errors corresponding to P_x and P_0 as $e\left(\boldsymbol{X},\boldsymbol{X}'\right)$ and $e\left(\boldsymbol{X},\mathbf{0}\right)$, respectively.

The average number of bit errors corresponding to $\left(\boldsymbol{p}_i^k\to\boldsymbol{p}_j^k\right)$ may then be computed by

$$\begin{aligned}e_t\left(\boldsymbol{p}_i^k,\boldsymbol{p}_j^k\right)&=e_i\left(\boldsymbol{p}_i^k,\boldsymbol{p}_j^k\right)+\frac{d_{i,j}}{N_a\left(Q\cdot\mathcal{L}\right)}\sum_{\boldsymbol{X}}e\left(\boldsymbol{X},\mathbf{0}\right)\\&\quad+\frac{\left(N_a-d_{i,j}\right)}{N_a\left(Q\cdot\mathcal{L}\right)\left(Q\cdot\mathcal{L}-1\right)}\sum_{\boldsymbol{X}}\sum_{\boldsymbol{X}'}e\left(\boldsymbol{X},\boldsymbol{X}'\right).\end{aligned} \tag{25}$$

Using the relation $b_2=\left\lfloor\log_2\binom{N_b}{N_a}\right\rfloor$, the BEP corresponding to the error event of $\left(\boldsymbol{p}_i^k\to\boldsymbol{p}_j^k\right)$ is then expressed as

$$P_{b,IC}=\frac{1}{2^{b_2}\left(\binom{N_b}{N_a}-1\right)}\sum_{i=1}^{2^{b_2}}\sum_{j=1\,(j\neq i)}^{\binom{N_b}{N_a}}(P_0)^{d_{i,j}}\ e_t\left(\boldsymbol{p}_i^k,\boldsymbol{p}_j^k\right). \tag{26}$$

On the other hand, when the SAP of a subblock is correctly detected, the codewords corresponding to the individual subcarriers may still be decoded incorrectly resulting in a PEP P_x. The probability of correctly detecting the subcarrier activation pattern may be expressed as

$$P_C=1-\sum_{i=1}^{2^{b_2}}\sum_{j=1\,(j\neq i)}^{\binom{N_b}{N_a}}(P_0)^{d_{i,j}} \tag{27}$$

and the BEP under this scenario is then given by

$$P_{b,C}=\frac{N_a\log_2\left(Q\cdot\mathcal{L}\right)P_C\sum_{\boldsymbol{X}}\sum_{\boldsymbol{X}'}P_x e\left(\boldsymbol{X},\boldsymbol{X}'\right)}{\left(Q\cdot\mathcal{L}\right)\left(Q\cdot\mathcal{L}-1\right)\left\{N_a\log_2\left(Q\cdot\mathcal{L}\right)+\left\lfloor\log_2\binom{N_b}{N_a}\right\rfloor\right\}}. \tag{28}$$

The overall BEP of the system may thus be formulated as

$$P_b=P_{b,IC}+P_{b,C}, \tag{29}$$

where $P_{b,IC}$ and $P_{b,C}$ are given by (26) and (28), respectively.

The overall BEP expressed by (29) depends on a number of parameters, namely the SNR, the modulation order $\mathcal{L}$, the number of DMs Q, the number of parallel subblocks K and the subcarrier activation ratio given by $r=N_a/N_b$ [29]. Different mapping methods between the information bits and the SAP may lead to different BEP performance of the proposed scheme [30]. As mentioned in [29], when the subcarrier activation ratio r is around 0.5, then there are many SAP and according to (24) and (26), the value of $P_{b,IC}$ is small. The value of $P_{b,IC}$ increases as r approaches 0 or 1. Nevertheless, it is seen from (22) and (26) that the value of $P_{b,IC}$ is vanishingly low at high SNR. On the other hand, $P_{b,C}$ may be reduced by using a smaller value of r for a given N_b and $\mathcal{L}$. Additionally, for a given r, a larger value of N_b increases $P_{b,C}$. Furthermore, large values of $\mathcal{L}$ and Q are

Authorized licensed use limited to: Khulna University. Downloaded on October 17,2026 at 10:20:16 UTC from IEEE Xplore. Restrictions apply.

not preferred, because these may degrade the error performance of the scheme [7], [30]. In a nutshell, it is recommended to usually adopt small values of N_b, N_a, Q and $\mathcal{L}$ and to take the design guidelines of Section IV-B into consideration.

B. Design Guidelines

Consider the SIM-OFDM-STSK system based on STSK $(M, N, T, Q, \mathcal{L})$ and SIM (N_b, N_a, K). The design guidelines for the system may be summarized as follows:

1) For all the possible $(\mathcal{L}, Q)$ combinations of the STSK system, the Q DMs are computed by either the capacity-optimal or the PEP-optimal design procedure [7], [12].
2) The number of subcarriers for the scheme has to be so chosen [8] that the symbols under each subcarrier experience frequency-flat fading. The length of the CP must also be greater than the channel's delay spread.
3) The maximum achievable rate of SIM-OFDM-STSK is greater than that of the classic OFDM-aided STSK, i.e. $R^{\max} > \frac{1}{T}\log_2(Q \cdot \mathcal{L})$, iff the system is so designed [20] that $N_b \geq 2(Q \cdot \mathcal{L})$.

Equation (14) may be written as [20], [23]

$$R = \frac{KN_b}{N_c T}\log_2(Q \cdot \mathcal{L}) + \frac{K}{N_c T}\left\lfloor \log_2 \binom{N_b}{N_a} \right\rfloor - \frac{K}{N_c T}(N_b - N_a)\log_2(Q \cdot \mathcal{L}). \tag{30}$$

When $N_a = (N_b - 1)$, we have from (30),

$$R = \frac{\log_2(Q \cdot \mathcal{L})}{T} + \frac{K}{N_c T}\lfloor \log_2 N_b \rfloor - \frac{K}{N_c T}\log_2(Q \cdot \mathcal{L}). \tag{31}$$

Again, $N_b \geq 2(Q \cdot \mathcal{L})$ gives $\lfloor \log_2 N_b \rfloor > \log_2(Q \cdot \mathcal{L})$. Hence $R > \frac{1}{T}\log_2(Q \cdot \mathcal{L})$, which indicates that the maximum achievable rate of SIM-OFDM-STSK is greater than that of the classic-OFDM STSK system when $N_b \geq 2(Q \cdot \mathcal{L})$.

On the other hand, when $N_b < 2(Q \cdot \mathcal{L})$, we have

$$\log_2 N_b < 1 + \log_2(Q \cdot \mathcal{L}). \tag{32}$$

Using (32) and the relation $\binom{N_b}{N_a} < \frac{N_b^{N_b - N_a}}{2^{N_b - N_a - 1}}$, we have [20]:

$$\left\lfloor \log_2 \binom{N_b}{N_a} \right\rfloor \leq (N_b - N_a)\log_2(Q \cdot \mathcal{L}). \tag{33}$$

Substituting (33) in (30), we have $R \leq \frac{1}{T}\log_2(Q \cdot \mathcal{L})$. Thus, the achievable rate of SIM-OFDM-STSK may be higher than that of the classic OFDM-STSK, only when $N_b \geq 2(Q \cdot \mathcal{L})$.

V. Numerical Results

In this section, SIM-OFDM-STSK is numerically characterized in terms of its BEP, achievable rate and complexity.

A. BEP

The BEP of the SIM-OFDM-STSK scheme is investigated for the COST207-TU12 channel model having a normalized Doppler frequency of $f_d = 0.01$. The main simulation parameters for this investigation are listed in Table III.

TABLE III
Main Simulation Parameters

Channel model	COST207-TU12
Fast fading envelope	Rayleigh
Normalized Doppler frequency, f_d	0.01
No. of subcarriers, N_c	64/256/512
CP length	32
No. of AE at transmitter, M	2
No. of AE at receiver, N	2
No. of transmit time slots, T	2
No. of DMs, Q	2,/4
Modulation order, $\mathcal{L}$	2/ 4
Number of parallel blocks	4/8/16

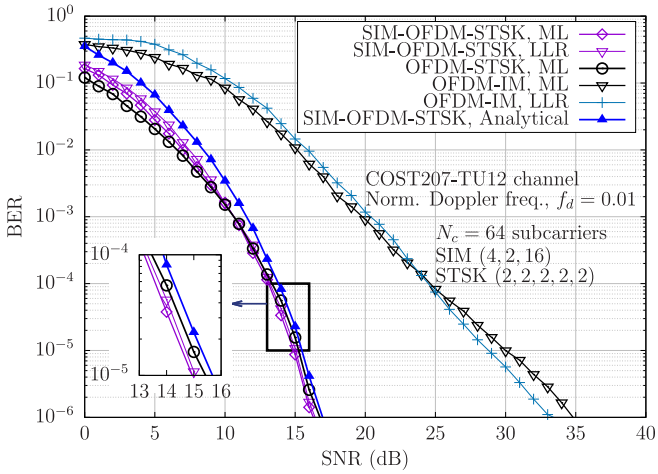


Fig. 3. Performance of the SIM $(4, 2, 16)$-OFDM-STSK $(2, 2, 2, 2, 2)$ system in dispersive channel employing both the ML detector and the soft-decision LLR detector, as compared to the classic SIM-OFDM system.

Fig. 3 portrays the BEP of the SIM $(4, 2, 16)$-OFDM STSK $(2, 2, 2, 2, 2)$ system employing both the ML detector and the soft-decision LLR detector. An exhaustive search based DM optimization [7], [8] was employed for minimizing the PEP among all the legitimate codewords and the $M \times T$ zero matrix. The performance of SIM-OFDM-STSK is also compared to that of the classic OFDM-STSK scheme. It is demonstrated in Fig. 3 that SIM-OFDM-STSK outperforms the classic OFDM STSK especially at high SNR. This is achieved due to the improved distance property of the index bits [2] at high-SNR region. The LLRs of the soft-decision detector are expressed in terms of the ML metric of the Euclidean distance between any two of the legitimate ST codewords. Consequently, the soft-decision LLR detector exhibits the same integrity of the ML detector. Additionally, the classic SIM-OFDM scheme is benefited neither by the multiple-antenna architecture of STSK nor by the DM optimization. As a result, the performance of the SIM-OFDM-STSK system is much more improved than that of the classic SIM-OFDM.

Authorized licensed use limited to: Khulna University. Downloaded on October 17,2026 at 10:20:16 UTC from IEEE Xplore. Restrictions apply.

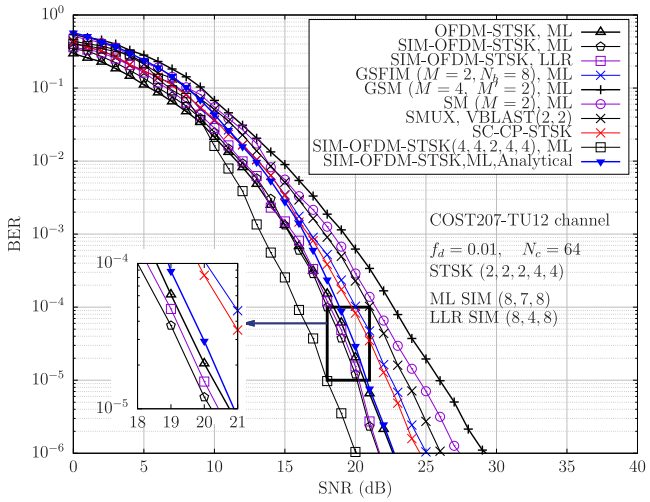


Fig. 4. Performance of the SIM-OFDM-STSK $(2, 2, 2, 4, 4)$ system in COST207-TU12 channel employing SIM $(8, 7, 8)$ for the ML detector and SIM $(8, 4, 8)$ for the LLR detectors. The performance is also compared to that of the state-of-the-art schemes.

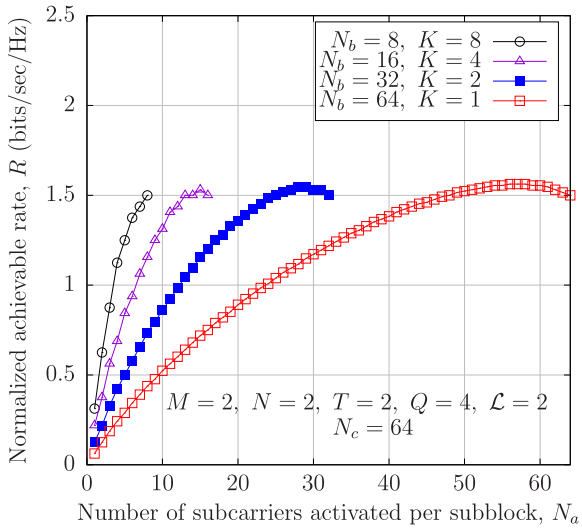


Fig. 5. Normalized achievable rate R of the SIM-OFDM-STSK scheme of Fig. 1 as a function of the number N_a of subcarriers activated.

The performance of the SIM $(8, 7, 8)$-OFDM-STSK $(2, 2, 2, 4, 4)$ employing the ML detector is investigated in Fig. 4. In order to impose the constraint of $N_a = N_b/2$ for the reduced-complexity LLR detector as mentioned in Section II-C2, we have considered a SIM $(8, 4, 8)$ for the soft-decision detector in place of SIM $(8, 7, 8)$ for the ML detector. Furthermore, the simulated performance of the SIM-OFDM-STSK (2, 2, 2, 4, 4) system is compared to the relevant benchmark schemes of cyclic prefixed single carrier STSK (CP-SC-STSK) scheme of [31], SM, GSM, SMUX and GSFIM. The detection technique of CP-SC-STSK scheme relies on the frequency-domain equalization (FDE) and the detection procedure as proposed in [22]. Both [31] and [22] employ minimum mean-squared error (MMSE) based FDE. It is well known that MMSE-based detector cannot outperform the ML detector in terms of BEP. As a result, the SIM-OFDM-STSK scheme exhibits an improved BEP compared to that of the CP-SC-STSK scheme of [31]. To investigate the effect of the number of transmit and receive AEs on the achievable performance, the SIM-OFDM-STSK $(4, 4, 2, 4, 4)$ system has also been studied in Fig. 4. Please note that the diversity order of the scheme in a full-rank and in a rank-deficient scenario is expressed by $d_{\text{full-rank}} = N \cdot \min(M, T)$ and $d_{\text{rank-deficient}} < N \cdot \min(M, T)$, respectively [7], [12]. Thus the SIM-OFDM-STSK $(4, 4, 2, 4, 4)$ system has a higher diversity order than that of the SIM-OFDM-STSK $(2, 2, 2, 4, 4)$ system, which is also evidenced by the simulation results. The simulated performance of the SIM-OFDM-STSK system is also compared to the analytical upper bound of the BEP of (29). Observe in Fig. 3 and Fig. 4 that the simulation results corroborate the analytical results.

Furthermore, the incorporation of SIM-OFDM with STSK makes the transmit codewords sparse in FD. As a result, advanced signal processing based detection algorithms, for example compressed sensing [21], [32], [33], matching pursuits [34], may be used for substantially improving the performance of the system. This study, however, is out of the scope of the present paper.

B. Achievable Rate

Fig. 5 illustrates the normalized achievable rate R of the SIM-OFDM-STSK scheme as expressed by (14) employing $N_c = 64$ subcarriers. It is observed that SIM-OFDM-STSK is capable of achieving normalized transmission rate higher than that achievable with the classic OFDM-aided STSK using lower number of subcarriers. This is achievable when the number of subcarriers per subblock N_b is so chosen that $N_b \geq 2\,(Q \cdot \mathcal{L})$, as mentioned in the design guidelines of Section IV-B. As shown in Fig. 5, the number of subcarriers activated which maximizes R is 56 and the maximum normalized transmission rate $R^{\max} = 1.55$, which denotes a 3.33% gain in achievable rate at a 25% reduction in the subcarriers utilized when $(Q \cdot \mathcal{L}) = 8$.

Fig. 6 illustrates the upper and lower bounds on the normalized achievable rate R of the SIM-OFDM-STSK system as given by (15) and (16) in conjunction with the actual normalized achievable rate R obtained from (14). Furthermore, Fig. 7 shows the bounds on the maximum normalized achievable rate $R^{\max}$ of the SIM-OFDM-STSK system given by (17) and (18) along with the actual maximum achievable rate $R^{\max}$, which is obtained by plotting (14). As seen from Fig. 6, the achievable rate R obtained from (14) is tightly upper- and lower-bounded by (15) and (16), respectively. Similarly, the maximum normalized achievable rate $R^{\max}$ of the SIM-OFDM-STSK system is also shown in Fig. 7 to be upper- and lower-bounded by (17) and (18), respectively.

The normalized achievable rate R of SIM-OFDM-STSK is compared to that of the relevant existing schemes in Fig. 8. It is

Authorized licensed use limited to: Khulna University. Downloaded on October 17,2026 at 10:20:16 UTC from IEEE Xplore. Restrictions apply.

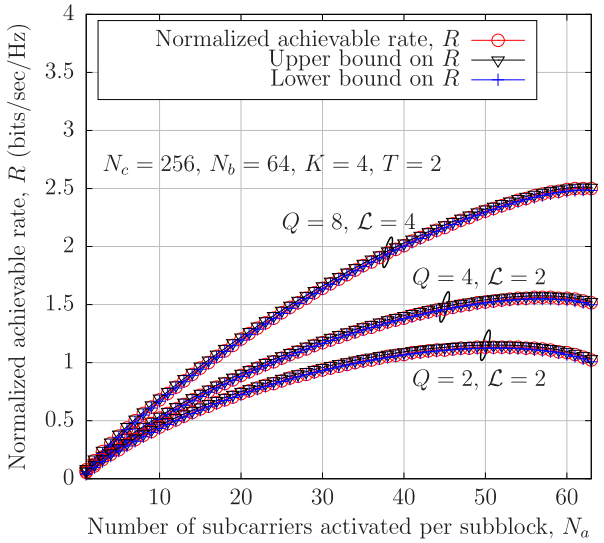


Fig. 6. The upper and lower bounds on the normalized achievable rate R of the SIM-OFDM-STSK are shown along with the actual achievable rate.

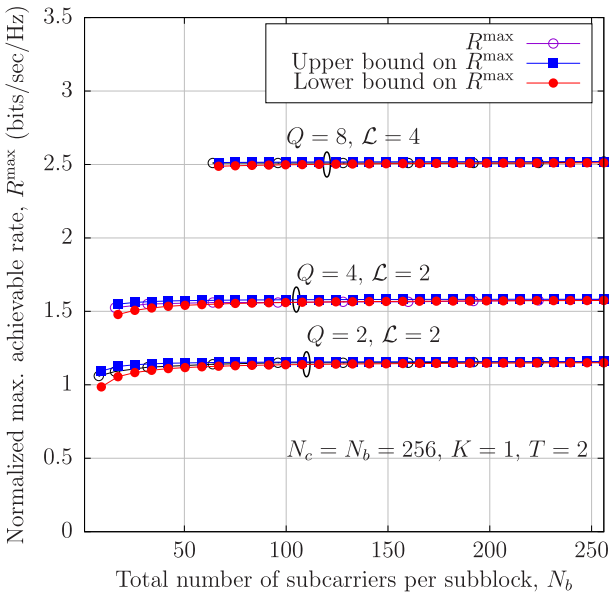


Fig. 7. The upper and lower bounds on the maximum normalized achievable rate $R^{\max}$ of the SIM-OFDM-STSK with $N_c = 256$ are plotted in conjunction with the actual maximum achievable rate $R^{\max}$.

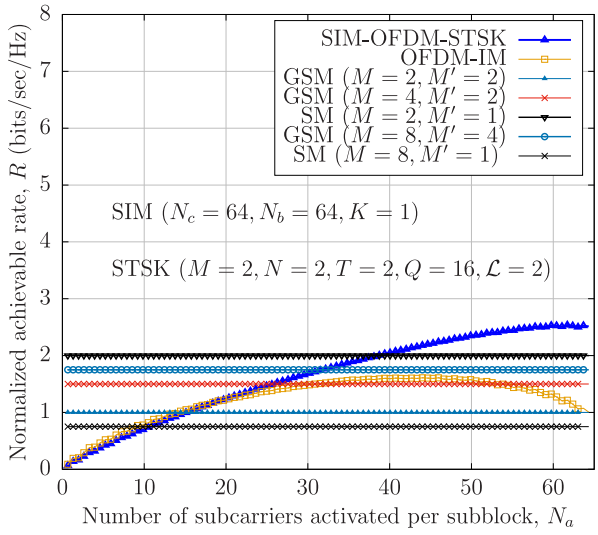


Fig. 8. Normalized achievable rate R as a function of N_a.

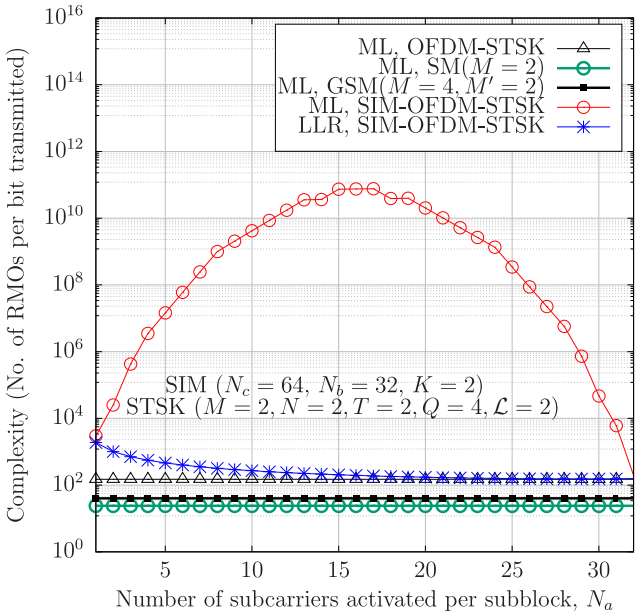


Fig. 9. Complexity associated with the relevant detectors in terms of the RMOs per bit of information transmitted.

observed that SIM-OFDM-STSK is capable of achieving higher transmission rate than that of the benchmark schemes.

C. Complexity

In order to compare the computational complexity imposed by the detectors, the decoding complexity is portrayed in Fig. 9 as a function of the number N_a of subcarriers activated. The computational complexity of the detectors is evaluated in terms of the RMOs required per bit of information transmitted. As seen in Fig. 9, the SM system imposes the lowest complexity. The complexity of the ML detector of classic-OFDM aided STSK does not vary with N_a. The ML detector of (10) is seen to impose a high decoding complexity when approximately 50% of the total subcarriers are activated. Under this condition, the scheme, however, is mostly benefited by the index bits or the bits mapped to the subcarrier indices. Observe that the complexity of the detector reduces to that of the classic-OFDM aided system where all the available subcarriers are activated. Furthermore, the reduced-complexity detector is readily available for SIM-OFDM-STSK in order to compensate the high complexity associated with the ML detector. The reduced-complexity detector, as seen from Fig. 9, imposes the same complexity of the classic-OFDM aided STSK without any compromise in performance, particularly when large number N_a of subcarriers are activated.

Authorized licensed use limited to: Khulna University. Downloaded on October 17,2026 at 10:20:16 UTC from IEEE Xplore. Restrictions apply.

VI. Conclusions

In this paper, a SIM-OFDM aided STSK system has been proposed and its achievable rate as well as performance has been investigated. Some helpful design guidelines have also been provided. The system exhibits an improved performance and provides additional bandwidth efficiency by employing subcarrier indices as information-bearing entity. Additionally, the normalized achievable rate has been observed to be higher than that of the classic OFDM aided STSK, when the design guidelines are followed. The SIM-OFDM based STSK system is capable of striking an appealing compromise among the achievable rate, performance and the decoding complexity.

References

[1] P. K. Frenger and N. A. B. Svensson, "Parallel combinatory OFDM signaling," *IEEE Trans. Commun.*, vol. 47, no. 4, pp. 558–567, Apr. 1999.

[2] E. Başar, Ü. Aygölü, E. Panayirci, and H. V. Poor, "Orthogonal frequency division multiplexing with index modulation," *IEEE Trans. Signal Process.*, vol. 61, no. 22, pp. 5536–5549, Nov. 2013.

[3] E. Basar, "On multiple-input multiple-output OFDM with index modulation for next generation wireless networks," *IEEE Trans. Signal Process.*, vol. 64, no. 15, pp. 3868–3878, Aug. 2016.

[4] R. Abu-alhiga and H. Haas, "Subcarrier-index modulation OFDM," in *Proc. IEEE Int. Symp. Pers., Indoor, Mobile Radio Commun.*, Sep. 2009, pp. 177–181.

[5] N. Ishikawa, S. Sugiura, and L. Hanzo, "Subcarrier-index modulation aided OFDM — Will it work?" *IEEE Access*, vol. 4, pp. 2580–2593, May 2016.

[6] M. Wen, E. Basar, Q. Li, B. Zheng, and M. Zhang, "Multiple-mode orthogonal frequency division multiplexing with index modulation," *IEEE Trans. Commun.*, vol. 65, no. 9, pp. 3892–3906, Sep. 2017.

[7] S. Sugiura, S. Chen, and L. Hanzo, "Coherent and differential space-time shift keying: A dispersion matrix approach," *IEEE Trans. Commun.*, vol. 58, no. 11, pp. 3219–3230, Nov. 2010.

[8] M. I. Kadir, S. Sugiura, S. Chen, and L. Hanzo, "Unified MIMO-Multicarrier designs: A space-time shift keying approach," *IEEE Commun. Surveys Tuts.*, vol. 17, no. 2, pp. 550–579, Second Quarter 2015.

[9] G. Foschini, G. Golden, R. Valenzuela, and P. Wolniansky, "Simplified processing for high spectral efficiency wireless communication employing multi-element arrays," *IEEE J. Sel. Areas Commun.*, vol. 17, no. 11, pp. 1841–1852, Nov. 1999.

[10] V. Tarokh, H. Jafarkhani, and A. Calderbank, "Space-time block codes from orthogonal designs," *IEEE Trans. Inf. Theory*, vol. 45, no. 5, pp. 1456–1467, Jul. 1999.

[11] B. Hassibi and B. M. Hochwald, "High-rate codes that are linear in space and time," *IEEE Trans. Inf. Theory*, vol. 48, no. 7, pp. 1804–1824, Jul. 2002.

[12] R. W. Heath and A. J. Paulraj, "Linear dispersion codes for MIMO systems based on frame theory," *IEEE Trans. Signal Process.*, vol. 50, no. 10, pp. 2429–2441, Oct. 2002.

[13] R. Mesleh, H. Haas, S. Sinanovic, C. W. Ahn, and S. Yun, "Spatial modulation," *IEEE Trans. Veh. Technol.*, vol. 57, no. 4, pp. 2228–2241, Jul. 2008.

[14] J. Jeganathan, A. Ghrayeb, L. Szczecinski, and A. Ceron, "Space shift keying modulation for MIMO channels," *IEEE Trans. Wireless Commun.*, vol. 8, no. 7, pp. 3692–3703, Jul. 2009.

[15] L. Zheng and D. N. C. Tse, "Diversity and multiplexing: A fundamental tradeoff in multiple-antenna channels," *IEEE Trans. Inf. Theory*, vol. 49, no. 5, pp. 1073–1096, May 2003.

[16] J. Li, M. Wen, X. Cheng, Y. Yan, S. Song, and M. H. Lee, "Generalized precoding-aided quadrature spatial modulation," *IEEE Trans. Veh. Technol.*, vol. 66, no. 2, pp. 1881–1886, Feb. 2017.

[17] L. Xiao *et al.*, "Compressed-sensing assisted spatial multiplexing aided spatial modulation," *IEEE Trans. Wireless Commun.*, vol. 17, no. 2, pp. 794–807, Feb. 2018.

[18] A. Younis, N. Serafimovski, R. Mesleh, and H. Haas, "Generalised spatial modulation," in *Proc. Asilomar Conf. Signals, Syst. Comput.*, Nov. 2010, pp. 1498–1502.

[19] S. Sugiura, S. Chen, and L. Hanzo, "Generalized space-time shift keying designed for flexible diversity-, multiplexing- and complexity-tradeoffs," *IEEE Trans. Wireless Commun.*, vol. 10, no. 4, pp. 1144 –1153, Apr. 2011.

[20] T. Datta, H. S. Eshwaraiah, and A. Chockalingam, "Generalized space-and frequency index modulation," *IEEE Trans. Veh. Technol.*, vol. 65, no. 7, pp. 4911–4924, Jul. 2016.

[21] S. Lu, I. A. Hemadeh, M. El-Hajjar, and L. Hanzo, "Compressed sensing-aided space-time frequency index modulation," *IEEE Trans. Veh. Technol.*, vol. 67, no. 7, pp. 6259–6271, Jul. 2018.

[22] M. I. Kadir, S. Sugiura, J. Zhang, S. Chen, and L. Hanzo, "OFDMA/SC-FDMA aided space-time shift keying for dispersive multiuser scenarios," *IEEE Trans. Veh. Technol.*, vol. 62, no. 1, pp. 408–414, Jan. 2013.

[23] M. I. Kadir, "Generalized space-time-frequency index modulation," *IEEE Commun. Lett.*, vol. 23, no. 2, pp. 250–253, Feb. 2019.

[24] Z. Liu, Y. Xin, and G. B. Giannakis, "Space-time-frequency coded OFDM over frequency-selective fading channels," *IEEE Trans. Signal Process.*, vol. 50, no. 10, pp. 2465–2476, Oct. 2002.

[25] P. Robertson, E. Villebrun, and P. Hoeher, "A comparison of optimal and sub-optimal MAP decoding algorithms operating in the log domain," in *Proc. IEEE Int. Conf. Commun.*, Jun. 1995, vol. 2, pp. 1009–1013.

[26] M. Wen, X. Cheng, M. Ma, B. Jiao, and H. V. Poor, "On the achievable rate of OFDM with index modulation," *IEEE Trans. Signal Process.*, vol. 64, no. 8, pp. 1919–1932, Apr. 2016.

[27] J. Stirling, *The Differential Method: A Treatise of the Summation and Interpolation of Infinite Series*. Akron, OH, USA: E. Cave, 1749.

[28] V. Tarokh, N. Seshadri, and A. Calderbank, "Space-time codes for high data rate wireless communication: Performance criterion and code construction," *IEEE Trans. Inf. Theory*, vol. 44, no. 2, pp. 744–765, Mar. 1998.

[29] A. I. Siddiq, "Effect of subcarrier activation ratio on the performance of OFDM-IM over Rayleigh fading channel," *IEEE Commun. Lett.*, vol. 21, no. 6, pp. 1293–1296, Jun. 2017.

[30] M. Wen, Y. Zhang, J. Li, E. Basar, and F. Chen, "Equiprobable subcarrier activation method for OFDM with index modulation," *IEEE Commun. Lett.*, vol. 20, no. 12, pp. 2386–2389, Dec. 2016.

[31] T. F. Rahman, A. Habib, C. Sacchi, and M. El-Hajjar, "Mm-wave STSK-aided single carrier block transmission for broadband networking," in *Proc. IEEE Symp. Comput. Commun.*, Jul. 2017, pp. 507–514.

[32] D. L. Donoho, "Compressed sensing," *IEEE Trans. Inf. Theory*, vol. 52, no. 4, pp. 1289–1306, Apr. 2006.

[33] H. Zhang, L. L. Yang, and L. Hanzo, "Compressed sensing improves the performance of subcarrier index-modulation-assisted OFDM," *IEEE Access*, vol. 4, pp. 7859–7873, Oct. 2016.

[34] S. G. Mallat and Z. Zhang, "Matching pursuits with time-frequency dictionaries," *IEEE Trans. Signal Process.*, vol. 41, no. 12, pp. 3397–3415, Dec. 1993.



Mohammad Ismat Kadir received the B.Sc.(Eng.) degree (first class) in electrical and electronic engineering and the M.Sc.(Eng.) degree in computer engineering from Bangladesh University of Engineering and Technology, Dhaka, Bangladesh, in 1992 and 1999, respectively, and the Ph.D. degree in electronics and electrical engineering from the University of Southampton, Southampton, U.K., in 2014. He is currently a faculty member with the Electronics and Communication Engineering Discipline, Khulna University, Khulna, Bangladesh. He was a Visiting Fellow with the School of ECS, University of Southampton, Southampton, U.K., from November 2016 to September 2017. His research interests include multicarrier systems, space-time coding, cooperative communications, millimeter-wave communications, and heterogeneous networks. He received the Commonwealth Scholarship from the Commonwealth Scholarship Commission, U.K.

Authorized licensed use limited to: Khulna University. Downloaded on October 17,2026 at 10:20:16 UTC from IEEE Xplore. Restrictions apply.